Modeling and Investigating the Dynamics of Hydraulic Telescopic Truck Cranes

Duc Hieu Tran[1], Sy Nam Nguyen[2*], Xuan Cuong Nguyen[1]

[1] Faculty of Mechanical Engineering, Hanoi University of Civil Engineering, Haibatrung, Hanoi, Vietnam

[2] Faculty of Civil and Industrial Construction, Hanoi University of Civil Engineering, Haibatrung, Hanoi, Vietnam

* Corresponding author's e-mail: namns@huce.edu.vn

ABSTRACT

The article deals with the problem of a dynamic model of the truck crane considering the elasticity of the rope and the ground. The dynamic model of a truck crane in the vertical plane has been established. When considering the oscillation of a truck crane, it is a dynamic system with a large number of degrees of freedom. This model will allow us to evaluate the dynamic response of the machine, analyze the vibration of the heavy object being lifted and lowered, and subsequently study stability and control problems. In this paper, the dynamic models of the cranes in the working plane have been established, built by Lagrange's multiplier Equations, which are systems of differential-algebraic Equations with the generalized coordinates of the machine's motions and the elastic coordinates. The Lagrange Equation provides a simple method for solving dynamic problems. The advantage of this Equation is that the form and number of Equations do not depend on the number of objects in the investigated system, nor do they depend on the way the objects move. The number of Lagrange Equations depends only on the number of degrees of freedom of the system.

Keywords: truck crane, dynamic models, elastic, Lagrange's multiplier Equations, differential – algebra.

INTRODUCTION

A truck crane is a lifting and transporting machine, serving as an important means of mechanizing production processes across all sectors of the national economy. With the rapid development of industry, the need to enhance labor productivity necessitates continuous development and improvement of crane technology. The construction industry relies heavily on cranes. High-rise buildings and large blocks cannot be constructed without mechanization of the lifting and transportation process. Fundamental changes in construction technology, such as the use of new materials and building blocks, have played a decisive role in transforming construction practices.

Similar to other cranes, a truck crane can lift, transport, and manipulate loads. This capability enlarges the workspace for the crane and allows for rapid relocation. The ability to perform various motions using different power units makes the truck crane a dynamic object. This dynamic nature, combined with the complexity of tasks and the involvement of multiple workers, increases the risk of accidents. These accidents can result in significant material losses and potentially harm workers.

The problem of modeling the dynamics of a truck crane is complex and requires the consideration of several factors in building the model. These factors include the fundamental and additional units of the crane, as well as the system encompassing most of the forces and masses involved

Dynamic analysis of truck cranes has been explored and reported in many works. Hong and Shah [1] studied the problem of dynamics and control of industrial cranes, including truck cranes. In their dynamic model, the stages are assumed to be rigid, and lifting motion is ignored. Abdel-Rahman et al. [2] introduced an overview of previous studies on this issue but did not mention the ground and cable distortion. Cekus et al. [3] proposed a mathematical model to analyze the movement of a load carried by a mobile crane, considering the influence of wind forces. Geisler and Sochacki [4], built a discrete-continuous model to investigate the vibration of truck cranes. The analytical solution is compared with the finite element results obtained using the COSMOS/M

package. The variations of the vibrational frequency versus the applied load and angles of boom lifting are graphically illustrated. Mijailović [5] developed a mechanical-mathematical model with eighteen general coordinates to analyze the dynamic response of truck cranes. Using the finite element method, Trąbka [6], presented various computational models with different numbers and selections of flexible components for a telescopic boom crane. The agreement between the numerical simulation outcomes and the test results of an actual structure was evaluated both qualitatively and quantitatively. Ilir and Naser [7] examined a model and simulation with MapleSim software and analyzed the dynamics and vibrations in truck-mounted cranes when lifting maximum loads. They also explored methods to control these vibrations and optimized the working process of truck-mounted cranes. Sagirli et al. [8] presented a theoretical model of a spatially driven telescopic rotating crane using the Linked Graph technique. Their model unifies the drive system and the main structure. However, the overall system exhibits high nonlinearity due to geometric nonlinearity, gyroscopic forces, hydraulic compressibility, and the elastic structure of the boom.

Raftoyiannis and Michaltsos [9] presented an analytical model suitable for the dynamic analysis of telescopic cranes. This model accounts for the time-varying nature of the second beam's natural frequency and shape. Their theoretical framework employed a sequential approach utilizing the modal superposition technique. Their team has analyzed various telescopic crane configurations, and the results are presented as dynamic response diagrams. Based on the energy method and the Hamilton principle, Liu et al. [10] established the parametric vibration Equation of the crane arm, which is expressed as the Mathieu Equation. Zheng and Wang [11] employed kinematic and dynamic modeling to analyze the movements of a telescopic crane, including slewing, luffing, telescoping, lifting, and pulling loads. Applying the Lagrange method, the crane dynamic Equations are obtained. These Equations along with the constraint Equation have form a system of differential-algebraic Equations (DAEs). The constraint stabilization method is then employed to solve these DAEs.

Maczynski and Wojciech [12] introduced a threedimensional (3D) model of a telescopic mobile crane, in which flexibilities and damping are considered. An algorithm for optimizing the drive functions of a crane's slewing upper structure is presented to determine the load positioning at the endpoint of a work cycle. Esqué et al. [13] introduced a new method for designing and testing mobile hydraulic cranes. They have created a modular system that can generate dynamic models of the crane and visualize the simulation in real time through a 3D interface. La Hera et al. [14] addressed control challenges in electro-hydraulic cranes (friction, dead zones, and vibrations) with a combined linear and nonlinear control algorithm, achieving accurate end effector tracking. Sochacki et al. [15] built a mathematical model for a telescopic boom and its hydraulic cylinder. They used Hamilton's principle to formulate the problem, considering the geometric nonlinearities involved. To solve this problem, they employed the small parameter method. Bold et al. [16] explored how various damping mechanisms affect the vibrations of a truck-mounted crane boom. When the boom extends or retracts, energy is lost due to two factors: the inherent damping properties of the materials used in the boom itself, and additional dampers strategically placed at the support and along the telescopic sections. Using the interactive analysis method, Qian et al. [17] determined outrigger reactions of a hydraulic mobile crane, to prevent potential outcomes during regular operation. Kacalak et al. [18] utilized intelligent computing methods to analyze and study crane simulations in operations. The model was designed within a CAD/CAE environment, enabling assessment of its stability for selected configurations and operating conditions. Neural network-assisted analysis of the various contact forces exerted by the outriggers on the ground, stability, torque, and center of mass during processing facilitates determining the trajectory to ensure crane stability. The results of the simulation study are presented in terms of the variation of stability conditions depending on different parameters. Based on the proposed dynamic computational method and finite element method (FEM), Sun et al. [19] used computer simulations with artificial intelligence to analyze crane stability during movements. A 3D model was created and analyzed for various configurations and loads. A neural network helped assess contact forces, torques, and center of mass to ensure stable crane operation. The simulations considered factors like boom and arm positions, load mass, and applied load value. Kjelland and Hansen [20] have introduced a method for actively controlling vibrations in the hydraulically operated boom of a vehicle loader crane, which is compared and combined with a pressure feedback control of the proportional valve

It is crucial to develop a dynamic model for the truck crane. The above studies have addressed crane dynamics in working scenarios but have not considered the elasticity of the cable and foundation.

Therefore, this study incorporates the elasticity of cables and foundations into the dynamic model of a truck crane to more accurately describe operating conditions and help design safer crane operations.

DYNAMIC MODEL OF TRUCK CRANE

Mechanical model

Truck cranes usually work in lifting mode, varying their reach or rotating around a vertical axis in the working plane. In this study, considering the case where the mechanism needs to work in a plane, the drum instead of the lifting rope will change the length of the lifting cable, and the boom can be changed in length or lifting angle by hydraulic cylinders as shown in Figure 1.

The outriggers resting on the elastic foundation. The system includes two types of elements: the front and rear support legs are modeled as the elastic element and the bumper element (c_1, b_1 and c_2, b_2). When the foundation is settled, the settlement of the foundation is represented as settlement parameters q_1 and q_2, respectively. Body 9 is considered a rigid block with a center of mass C_9. On the body of the vehicle is a slewing platform 8. The winch system 7 lifts and lowers the lifting object thanks to the motor torque M. The lifting cable in the working process is considered an elastic element with a stiffness coefficient of c, a drag coefficient of b and a total stretch is x_s. The lifting lever model is the reciprocating stages 3, 4, and 5 which are pushed by a hydraulic motor, on the top of the third segment is the hoist assembly 2. The lifting lever is raised and lowered by hydraulic cylinder 6. During the working process, the hydraulic cylinders will generate thrust to change the reach or lift angle of the boom. The above model of truck crane is a mixed system that has both a tree structure and a ring structure (forklift cluster). To build a dynamic model for this model, there are several methods, in which the Lagrange multiplier method is suitable [21]. The model is determined to consider rope elasticity and the ground, ignoring external influences such as wind and chassis elasticity. To build the dynamic model of the crane, some assumptions to simplify the problem are as follows:

- The chassis frame, which is the basic lifting element of the crane, rests on four extended stays based on a foundation.
- The rotational frame (body) 8, performs rotational movement towards the vertical axis (movement in rotational plane). In this paper, only the crane works in the plane, so the rotating part is fixed relative to the frame.
- Crane boom, rotationally mounted in the body, performing movement towards vertical axis (lifting plane) and movement of reciprocal extension of units (telescopic movement).
- The motor shaft, the hydraulic pump, the gearbox shafts and gears, and the joints are stiff.
- The boom of the crane is uniform over the entire length and is stiff.
- The cable has the reference hardness c, and the vibration quenching coefficient is b, omitting changes in the length of the cable length from the boom to the drum due to the influence of the angle of rotation.
- The lifting cylinder should be replaced with a spring and shock absorber equivalent, ignoring the mass of the piston-cylinder during service.
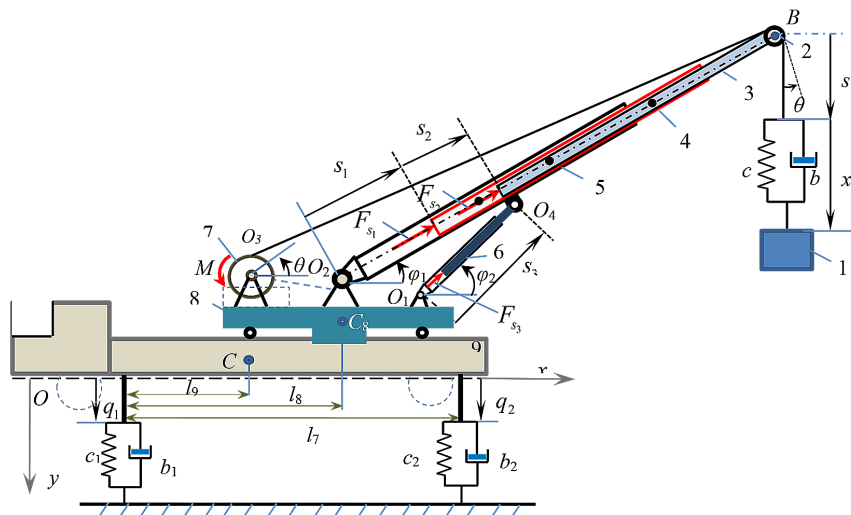- The influence of wind load is ignored.

Figure 1. Model of truck crane in the working plane

Equations of motion

Choose interpolation coordinates and linkage equations

Figure 1 diagram, we have the parameters and choose the coordinates as follows: Weight 1 is the load to be lifted when working, the mass of the lifting object and the hook is m_1. For O_2B consisting of three bars, consider rods 3, 4, and 5 as uniform cross-sectional bars with the center of mass, and length of C_3, C_4, C_5, m_3, m_4, m_5 and l_3, l_4, l_5, respectively. The lever with O_2B has a variable lift angle thanks to hydraulic cylinder 6 with variable length s_3 due to thrust F_{s_3} (initially long cylinder l_5, ignoring cylinder weight). Winch 7 rotates around the O_3 axis to collect or release the rope. Assume that the winch drum and the rope wrapped around it weight m_7, and radius r_7. The slewing platform 8 has a mass m_8, the center of mass C_8 carrying the actuator rotates around the body. In the working mode in the plane under consideration, the slewing platform 8 is stationary relative to the body of the vehicle. The bodywork is modeled as part 9, with a center of mass and mass of C_9 and m_9, respectively.

To make the Equation of motion dynamics of the crane, we choose the interpolation coordinates as follows: q_1, q_2 is the settlement of the elastic foundation at each outrigger; s is the length of the rope from the tip of the boom to the rope hoist 1; φ_1, φ_2 is the lift angle of O_2B rod and cylinder 6, respectively; s_1, s_2 determines the relative reciprocating motion of segment 4 on boom segment 5 and rod segment 3 on boom segment 4 (the telescopic extension boom), respectively; s_3 is cylinder length 6; x_s is the elongation of the rope; θ is the swing angle of the lifting body.

Linkage Equations: The coordinate system selected above is a residual coordinate system because φ_1, φ_2 depends on s_3 the following linkage Equations:

$$\begin{cases} f_1 = l_6 \sin\varphi_1 - s_3 \sin\varphi_2 + l_7 \sin\alpha = 0 \\ f_2 = l_6 \cos\varphi_1 - s_3 \cos\varphi_2 + l_7 \cos\alpha = 0 \end{cases} \tag{1}$$

Determine the kinetic energy of the system

The kinetic energy of the system is equal to the sum of the kinetic energies of the solid bodies:

$$T = T_1 + T_2 + ... + T_9 \tag{2}$$

Body kinetic energy 9. When the ground is elastic, the body will move parallel to the plane as shown in Figure 2, we have kinetic energy:
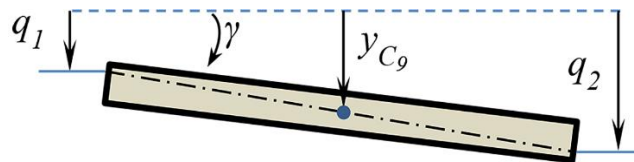

Figure 2. Body displacement

$$T_9 = 0.5 J_9 \omega_9^2 + 0.5 m_9 v_{C_9}^2 \tag{3}$$

where: J_9 is the moment of inertia of the body taken with its center of mass C_9, ω_9 is the angular velocity of the body, $\omega_9 = \dot\gamma$, v_{C_9} and is the velocity of the center of mass C_9. They are defined as follows:

$$\tan\gamma \approx \gamma = (q_2 - q_1)/l_7 \Rightarrow \dot\gamma = (\dot q_2 - \dot q_1)/l_7 \tag{4}$$

$$y_{C_9} = q_1 + l_9 \tan\gamma + constant \Rightarrow y_{C_9} = q_1 + l_9\gamma + constant$$
$$\Rightarrow v_{C_9} = \dot y_{C_9} = \dot q_1 + l_9\dot\gamma \tag{5}$$

Substituting (6), and (5) into (4), simplifying we get:

$$T_9 = 0.5\dot q_2^2 (J_9 + m_9 l_9^2)/l_7^2 + 0.5[J_9/l_7^2 + m_9(1-l_{97})^2]\dot q_1^2 - [J_9/l_7^2 - m_9 l_{97}(1-l_{97})]\dot q_1 \dot q_2 \tag{6}$$

where: $l_{97} = l_9/l_7$.

The kinetic energy of the slewing platform 8. The slewing platform is fixed to the chassis, so the kinetic energy is calculated as the chassis:

$$T_8 = 0.5 J_8 \omega_8^2 + 0.5 m_8 v_{C_8}^2 \tag{7}$$

where: m_8 and J_8 are the mass of the slewing platform and the moment of inertia of the slewing platform taken with its center of mass C_8, ω_8 is the angular velocity of the slewing platform, equal to the angular velocity of the body $\omega_8 = \dot{\gamma}$, v_{C_8} is the mass velocity center of the body, we have:

$$y_{C_8} = q_1 + l_8 \tan \gamma + constant \Rightarrow y_{C_8} = q_1 + l_8 \gamma = (l_8/l_7) q_2 + (1 - l_8/l_7) q_1 + constant \tag{8}$$

$$\Rightarrow v_{C_8} = \dot{y}_{C_8} = \dot{q}_1 + l_8 \dot{\gamma} = (l_8/l_7) \dot{q}_2 + (1 - l_8/l_7) \dot{q}_1 \tag{9}$$

Substituting the expression (9), (4) into (7) to simplify, we have the body kinetic energy:

$$T_8 = 0.5 (J_8 + m_8 l_8^2) \dot{q}_2^2 / l_7^2 + 0.5 [J_8/l_7^2 + m_8 (1 - l_{87})^2] \dot{q}_1^2 - [J_8/l_7^2 - m_8 l_{87} (1 - l_{97})] \dot{q}_1 \dot{q}_2 \tag{10}$$

where: $l_{87} = l_8/l_7$.

Kinetic energy is required with O_2B. Because the horizontal deviation of the O_2 bearing relative to the center of mass C_2 is negligible compared to the size l_7. Therefore, approximate the vertical displacement of the bearing O_2:

$$y_{O_2} = y_{C_8} + constant = q_1 + l_8 \gamma + constant \tag{11}$$

$$v_{O_2} = v_{C_8} = \dot{y}_{O_2} = \dot{y}_{C_8} = l_{87} \dot{q}_2 + (1 - l_{87}) \dot{q}_1 \tag{12}$$

We have the coordinates of the centroids of the segments needed:

$$
\begin{aligned}
x_{C_5} &= (l_5/2) \cos(\varphi_1 - \gamma) + constant & y_{C_5} &= y_{O_2} - (l_5/2) \sin(\varphi_1 - \gamma) \\
x_{C_4} &= (s_1 + l_4/2) \cos(\varphi_1 - \gamma) + constant & y_{C_4} &= y_{O_2} - (s_1 + l_4/2) \sin(\varphi_1 - \gamma) \\
x_{C_3} &= (s_1 + s_2 + l_3/2) \cos(\varphi_1 - \gamma) + constant & y_{C_3} &= y_{O_2} - (s_1 + s_2 + l_3/2) \sin(\varphi_1 - \gamma) \\
x_B &= (s_1 + s_2 + l_3) \cos(\varphi_1 - \gamma) + constant & y_B &= y_{O_2} - (s_1 + s_2 + l_3) \sin(\varphi_1 - \gamma)
\end{aligned}
\tag{13}
$$

Derivative (13) with time we can calculate the velocities of the centers of mass C_3, C_4, C_5, and tip B, along with the angular velocity:

$$\omega_{O_2B} = \dot{\varphi}_1 - \dot{\gamma} = \dot{\varphi}_1 - (\dot{q}_2 - \dot{q}_1)/l_7 \tag{14}$$

The kinetic energy of the objects from 2 to 5 of the cranes (both solid objects moving in parallel, and the kinetic energy of end B (as a concentrated mass) can be calculated as:

$$
\begin{aligned}
T_3 = &0.5 m_3 \dot{y}_{O_2}^2 + 0.5 m_3 (\dot{s}_1 + \dot{s}_2)^2 + 0.5 m_3 [(s_1 + s_2 + l_3/2)^2 + l_3^2/12] \times (\dot{\varphi}_1 - \dot{\gamma})^2 - m_3 \dot{y}_{O_2} (\dot{s}_1 + \dot{s}_2) \sin(\varphi_1 - \gamma) \\
&- m_3 (s_1 + s_2 + l_3/2) \dot{y}_{O_2} (\dot{\varphi}_1 - \dot{\gamma}) \cos(\varphi_1 - \gamma)
\end{aligned}
\tag{15}
$$

$$
\begin{aligned}
T_4 = &0.5 m_4 \dot{y}_{O_2}^2 + 0.5 m_4 \dot{s}_1^2 + 0.5 m_4 [(s_1 + l_4/2)^2 + l_4^2/12] \times (\dot{\varphi}_1 - \dot{\gamma})^2 - m_4 \dot{y}_{O_2} \dot{s}_1 \sin(\varphi_1 - \gamma) \\
&- m_4 (s_1 + l_4/2) \dot{y}_{O_2} (\dot{\varphi}_1 - \dot{\gamma}) \cos(\varphi_1 - \gamma)
\end{aligned}
\tag{16}
$$

$$T_5 = 0.5 m_5 \dot{y}_{O_2}^2 + m_5 l_5^2/6 (\dot{\varphi}_1 - \dot{\gamma})^2 - 0.5 m_5 l_5 \dot{y}_{O_2} (\dot{\varphi}_1 - \dot{\gamma}) \cos(\varphi_1 - \gamma) \tag{17}$$

$$T_2 = 0.5 m_2 \left(\begin{aligned} &\dot{y}_{O_2}^2 + (\dot{s}_1 + \dot{s}_2)^2 + (s_1 + s_2 + l_3)^2 (\dot{\varphi}_1 - \dot{\gamma})^2 - 2\dot{y}_{O_2} (\dot{s}_1 + \dot{s}_2) \sin(\varphi_1 - \gamma) \\ &- 2(s_1 + s_2 + l_3) \dot{y}_{O_2} (\dot{\varphi}_1 - \dot{\gamma}) \cos(\varphi_1 - \gamma) \end{aligned} \right) \tag{18}$$

where: $l_{47} = l_4/l_7$, $l_{57} = l_5/l_7$

The kinetic energy of lifting body 1:

$$T_1 = 0.5 m_1 v_1^2 + 0.5 J_1 \dot{\theta}^2 \tag{19}$$

where: J_1 is the moment of inertia of the mass about its center of mass. Since the O_2O_3 axis distance is very small compared to the O_2B distance, for simplicity we assume the length of the O_3B wire is equal to the O_2B rod. Let the length of wire from hanger B to hanger be s, so the total length of rope is:

$$s^* = l_5 + s_1 + s_2 + n_p s \text{ or } s = (s^* - l_5 - s_1 - s_2)/n_p \tag{20}$$

The long strain of the cable is x_s, we have the coordinates of the load:

$$x_1 = x_B + (s + x_s)\sin\theta = (s_1 + s_2 + l_3)\cos(\varphi_1 - \gamma) + (s + x_s)\sin\theta + constant \tag{21}$$

$$y_1 = y_B + (s + x_s)\cos\theta = y_{O_2} - (s_1 + s_2 + l_3)\sin(\varphi_1 - \gamma) + (s + x_s)\cos\theta \tag{22}$$

The time derivative of the expression (21), (22) we can determine v1, then instead of (19) we get:

$$\begin{aligned}
T_1 = 0.5 m_1 \big[& \dot{y}_{O_2}^2 + (\dot{s}_1 + \dot{s}_2)^2 + (\dot{s} + \dot{x}_s)^2 + (s_1 + s_2 + l_3)^2 (\dot{\varphi}_1 - \dot{\gamma})^2 \\
& -2(s_1 + s_2 + l_3)\dot{y}_{O_2}(\dot{\varphi}_1 - \dot{\gamma})\cos(\varphi_1 - \gamma) - 2(s + x_s)\dot{y}_{O_2}\dot{\theta}\sin\theta \\
& +2(\dot{s}_1 + \dot{s}_2)(\dot{s} + \dot{x}_s)\sin(\theta - \varphi_1 + \gamma) + 2(s + x_s)(\dot{s}_1 + \dot{s}_2)\dot{\theta}\cos(\theta - \varphi_1 + \gamma) \\
& -2(s_1 + s_2 + l_3)(\dot{s} + \dot{x}_s)(\dot{\varphi}_1 - \dot{\gamma})\cos(\theta - \varphi_1 + \gamma) \\
& +2(s_1 + s_2 + l_3)(s + x_s)\dot{\theta}(\dot{\varphi}_1 - \dot{\gamma})\sin(\theta - \varphi_1 + \gamma) \big] + 0.5 J_1 \dot{\theta}^2
\end{aligned} \tag{23}$$

Substituting the kinetic energy of the bodies into expression (2) we get the kinetic energy of the mechanical system:

$$\begin{aligned}
T = & 0.5(m_1 + m_2 + m_3 + m_4 + m_5)\dot{y}_{O_2}^2 + 0.5(m_1 + m_2 + m_3)(\dot{s}_1 + \dot{s}_2)^2 + 0.5 m_4 \dot{s}_1^2 + 0.5 m_1 (\dot{s} + \dot{x}_s)^2 \\
& + 0.5(m_1(s + x_s)^2 + J_1)\dot{\theta}^2 \\
& + 0.5 \begin{bmatrix} m_1(s_1 + s_2 + l_3)^2 + m_2(s_1 + s_2 + l_3)^2 + m_3((s_1 + s_2 + l_3/2)^2 + l_3^2/12) \\ + m_4((s_1 + l_4/2)^2 + l_4^2/12) + m_5 l_5^2/6 \end{bmatrix} \\
& \times (\dot{\varphi}_1 - \dot{\gamma})^2 + 0.5\left((J_8 + J_9)/l_7^2 + m_8 l_{87}^2 + m_9 l_{97}^2\right)\dot{q}_2^2 \\
& -(m_1 + m_2 + m_3)\dot{y}_{O_2}(\dot{s}_1 + \dot{s}_2)\sin(\varphi_1 - \gamma) \\
& + m_1 \dot{y}_{O_2}(\dot{s} + \dot{x}_s)\cos\theta - m_1(s + x_s)\dot{y}_{O_2}\dot{\theta}\sin\theta \\
& - \begin{bmatrix} (m_1 + m_2)(s_1 + s_2 + l_3) + m_3(s_1 + s_2 + l_3/2) \\ + m_4(s_1 + l_4/2) + m_5 l_5/2 \end{bmatrix}\dot{y}_{O_2}(\dot{\varphi}_1 - \dot{\gamma})\cos(\varphi_1 - \gamma) \\
& + m_1(\dot{s}_1 + \dot{s}_2)(\dot{s} + \dot{x}_s)\sin(\theta - \varphi_1 + \gamma) + m_1(s + x_s)(\dot{s}_1 + \dot{s}_2)\dot{\theta}\cos(\theta - \varphi_1 + \gamma) \\
& - m_1(s_1 + s_2 + l_3)(\dot{s} + \dot{x}_s)(\dot{\varphi}_1 - \dot{\gamma})\cos(\theta - \varphi_1 + \gamma) \\
& + m_1(s_1 + s_2 + l_3)(s + x_s)\dot{\theta}(\dot{\varphi}_1 - \dot{\gamma})\sin(\theta - \varphi_1 + \gamma) \\
& - m_4 \dot{y}_{O_2}\dot{s}_1 \sin(\varphi_1 - \gamma) + (m_8 l_{87}(1 - l_{87}) + m_9 l_{97}(1 - l_{97}) - (J_8 + J_9)/l_7^2)\dot{q}_1 \dot{q}_2
\end{aligned} \tag{24}$$

where: $\dot{\gamma} = (\dot{q}_2 - \dot{q}_1)/l_7$, $\dot{y}_{O_2} = l_{87}\dot{q}_2 + (1 - l_{87})\dot{q}_1$

Determining potential and generalized non-conservative forces

Rigidity factor of rope

When the rope is in tension with length L, the tensile stiffness is EF (where E is the elastic modulus of the rope material, F is the total cross-sectional area), stiffness coefficient c (N/m) is:

$$c = EF/L \tag{25}$$

Thus, from the expression, (25) we see that the stiffness of the rope is inversely proportional to the length of the wire. In case the length of rope from the first pulley to the hook has a multiple, the stiff less of this part is determined by the sum of the stiff less of the branches:

- Rigidity coefficient of rope from roller to hoist:

$$c_1 = EF/(l_5 + s_1 + s_2) \tag{26}$$

- The coefficient of stiffness of the rope from the hoist to the hanger with the hoist multiplier n_p is:

$$c_2 = n_p EF/s \tag{27}$$

- Rigidity factor equivalent to the whole rope:

$$1/c = 1/c_1 + 1/c_2 = (l_5 + s_1 + s_2)/(EF) + s/(n_p EF) \Rightarrow c = EF/(l_5 + s_1 + s_2 + s/n_p) \tag{28}$$

Potential energy

We have the potential energy of the mechanical system equal to the sum of the potential energy due to the gravity of the bodies and the potential energy of the springs:

$$\Pi = \Pi_{P_1} + \Pi_{P_2} + \Pi_{P_3} + \Pi_{P_4} + \Pi_{P_5} + \Pi_{P_8} + \Pi_{P_9} + \Pi_c + \Pi_{c_1} + \Pi_{c_2} \tag{29}$$

Substituting Equations from 26 to 28 into 29, shortening we get:

$$
\begin{aligned}
\Pi = &-(m_1 + m_2 + m_3 + m_4 + m_5)g y_{O_2} \\
&+ [(m_1 + m_2)(s_1 + s_2 + l_3) + m_3(s_1 + s_2 + l_3/2) + m_4(s_1 + l_4/2) + m_5 l_5/2]g \sin(\varphi_1 - \gamma) \\
&- m_1 g(s + x_s)\cos\theta - (m_8 + m_9)g q_1 - (m_8 l_8 + m_9 l_9)g\gamma \\
&+ 0.5 EF x_s^2/(l_5 + s_1 + s_2 + s/n_p) + 0.5 c_1 q_1^2 + 0.5 c_2 q_2^2 + constant
\end{aligned}
\tag{30}
$$

Generalized nonconservative forces

The non-potential operating forces on the mechanical system include: the force of the cylinders $\vec{F}_{s_1}, \vec{F}_{s_2}, \vec{F}_{s_3}$ acting on the fine lines; motor torque M acting on the shaft O_3; viscous drag $\vec{F}_b = -b\dot{x}, \vec{F}_{b_1} = -b_1\dot{q}_1, \vec{F}_{b_2} = -b_2\dot{q}_2$.

The total virtual work of the system is [21]:

$$\sum \delta A = F_{s_1}\delta s_1 + F_{s_2}\delta s_2 + F_{s_3}\delta s_3 + M\delta s^*/n_p R - b_1\dot{q}_1\delta q_1 - b_2\dot{q}_2\delta q_2 - b\dot{x}_s\delta x_s$$

So do we have generalizing forces:

$$
\begin{aligned}
Q_{s_1}^* = F_{s_1}, Q_{s_2}^* = F_{s_2}, Q_{s_3}^* = F_{s_3}, Q_s^* = M/n_p R, \\
Q_{q_1}^* = -b_1\dot{q}_1, Q_{q_2}^* = -b_2\dot{q}_2, Q_{x_s}^* = -b\dot{x}_s, Q_{\varphi_1}^* = 0, Q_{\varphi_2}^* = 0
\end{aligned}
\tag{31}
$$

Dynamic equations and solution methods

The Lagrange multiplier Equation is an Equation written for the residual generalized coordinate system, the Equation has the form [16]:

$$\frac{d}{dt}\left(\frac{\partial T}{\partial \dot{q}_k}\right) - \frac{\partial T}{\partial q_k} = -\frac{\partial \Pi}{\partial q_k} + Q_k^* - \sum_{i=1}^{r}\lambda_i \frac{\partial f_i}{\partial q_k}, (k = 1,2,...r) \tag{32}$$

where: r is the total number of residual generalized coordinates, q_k is the kth generalized coordinates, T is the kinetic energy, Π is the potential energy, Q_k^* is the non-potentially generalized force, f_i and the ith linkage Equation of the system.

Substituting the expressions (24), (30), (31) and (1) into Equations 32 the differential-algebraic Equations describing the motion of the system have the form [21]:

$$M(s)\ddot{s} + C(s,\dot{s})\dot{s} + g(s) = \tau(t) - \Phi_s^T(s)\lambda \tag{33}$$

$$f(s) = 0 \tag{34}$$

where: s is the vector of generalized coordinates, $M(s)$ is the generalized mass matrix of the system, $\tau(t)$ is the generalized force vector for non-potentially active forces, $\lambda = [\lambda_1, \lambda_2]^T$ is the vector of Lagrange multipliers, f is the constraint conditions, Φ_s is the Jacobi matrix of vector f, $C(s,\dot{s})$ is the matrix centrifugal inertia and Coriolis inertia, $g(s)$ is a generalized force vector corresponding to the forces acting as potential forces.

The system of Equations from 41 to 51 (Appendix) together with the two constraint Equations 1 forms a system of differential-algebraic Equations with the number of Equations equal to the unknowns being the generalized coordinates and multiplier Lagrange is λ_1, λ_2. In the case of ignoring the deformation, from the above system of Equations, we remove the Equations of the deformation coordinates, and at the same time give the strain zero in the remaining Equations, we will obtain a dynamic model for the structure. All solid stitches.

The system of Equations 33 and 34 is a system of differential-algebraic Equations written for a system with a ring structure. To solve this system of Equations, we have two groups of methods: the method of transforming algebraic differential Equations into ordinary Equations and the direct solution of differential-algebraic Equations.

For the convenience of writing, we denote.

$$p_1(s,\dot{s},t)=\tau(t)-C(s,\dot{s},t)\dot{s}-g(s) \tag{35}$$

Equations 33, 34 now take the form:

$$M(s)\ddot{s}+\Phi_s^T(s)\lambda=p_1(s,\dot{s},t) \tag{36}$$

$$f(s)=0 \tag{37}$$

Deriving twice Equation 37 we get the Equations

$$\dot{f}(s)=\frac{\partial f}{\partial s}\dot{s}=\Phi_s(s)\dot{s}=0 \tag{38}$$

$$\ddot{f}(s)=\Phi_s(s)\ddot{s}+\dot{\Phi}_s(s)\dot{s}=0 \Rightarrow \Phi_s\ddot{s}=-\dot{\Phi}_s(s)\dot{s}=p_2(s,\dot{s}) \tag{39}$$

Equations 36 and 39 can be rewritten as the following matrix:

$$\begin{bmatrix} M & \Phi_s^T \\ \Phi_s & 0 \end{bmatrix}\begin{bmatrix} \ddot{s} \\ \lambda \end{bmatrix}=\begin{bmatrix} p_1 \\ p_2 \end{bmatrix} \tag{40}$$

Equation 42 is proven to be equivalent to the system of Equations 35, and 36 in [21]. To solve Equation 42, we can use methods of decomposing the Lagrange factor and eliminating the Lagrange factor [21]. In this paper, algebraic differential Equations have been transformed into ordinary Equations, and then the Runge – Kutta 4th order method with numerical technique has been employed to solve the differential Equations.

CALCULATION

Data for calculation parameters are taken according to the truck crane 55713-1K as Table 1. The hardness of the ground is determined according to the following formula:

$$C_0=q_0.F$$

where: q_0 – coefficient of soil hardness as table 2; F – outrigger cushion contact area, $F = 0.45 \times 0.45 \text{m}^2$ Calculation results in a load of m_1=3.5tons. The hard coefficient of the ground is chosen to be the largest $q_0 = 100 \text{ MN/m}^3$, the resistance coefficient of the ground $b_1=b_2=405000$ Ns/m (0.1%) (Tab. 2).

Table 1. Loading characteristics of truck crane 55713-1K

Parameter	Value	Unit	Parameter	Value	Unit
m_1	3500	kg	l_3	7	m
m_2	178	kg	l_4	8	m
m_3	192.6	kg	l_5	9	m
m_4	192.6	kg	$l_6 = O_1O_2$	1.1	m
m_5	192.6	kg	l_7	3.08	m
m_6	96	kg	l_8	1.452	m
m_7	32	kg	l_9	0.56	m
m_8	4700	kg	J_8	763.18	kg/m²
m_9	10590	kg	J_9	15200.21	kg/m²

Table 2. Coefficient of specific resistance q_0 (MN/m³) of the ground

Characteristics of the land	Coefficient value q_0
Sand, wet clay, arable land	25 ÷ 35
Tight sand, wet clay	36 ÷ 60
Tight clay	100 ÷ 125
Hard pavement	130 ÷ 180

The influence of the boom length changes on the dynamic response of the crane. In case the heavy object is pushed away and at the same time lowered so that the height of the object remains constant, then the angle of inclination of the boom remains constant. So:
The angle of inclination of the boom is locked:

$$\varphi_1 = constant, \varphi_2 = constant, s_3 = constant \Rightarrow \dot\varphi_1 = \dot\varphi_2 = 0, \ddot\varphi_1 = \ddot\varphi_2 = 0$$

Problem: Given a known law of motion: s_1, s_2, and s. Find the movements: x_s, q_1, q_2, θ

Choose a known motion: Law of motion s_1 and s_2: the boom segments 3 and 4 are ejected from rest with acceleration with constant acceleration in the interval $[0, T_1]$, uniform motion in the interval $[T_1, T_2]$, slow motion, and stop with the same acceleration in the interval $[T_2, T_3]$, the law of motion:

$$v_1 = \begin{cases} a_1 t \text{ with } 0 \le t < T_1 \\ a_1 T_1 = V_{10} \text{ with } T_1 \le t < T_2 \\ V_{10} - a_1(t - T_2) \text{ with } T_2 \le t < T_3 \text{ and } T_3 = T_2 + T_1 \end{cases} \quad ; \quad v_2 = \begin{cases} a_2 t \text{ with } 0 \le t < T_1 \\ a_2 T_1 = V_{20} \text{ with } T_1 \le t < T_2 \\ V_{20} - a_2(t - T_2) \text{ with } T_2 \le t < T_3 \end{cases}$$

- Length of the boom before and after the lever is pushed out: $L_{min} = 10.5$ m; $L_{max} = 22.4$ m
- The tilt angle of the boom: $\varphi_1 = 60^o$
- The rate of change needs to be steady: $V_{10} = V_{20} = 0.35$ m/s

Law of motion s of the mass: Load 1 is lowered with speed v such that its height remains constant.

$$v = \begin{cases} at \text{ with } 0 \le t < T_1 \\ a T_1 = V_0 \text{ with } T_1 \le t < T_2 \\ V_{10} - a(t - T_2) \text{ with } T_3 = T_2 + T_1 \text{ and } T_2 \le t < T \end{cases}$$

Length of rope $s(0) = s_0 = 9.09$ m. Choose the law of motion that does not change the height of the weight.
- Initial conditions: The Equation of motion of the system in this case x_s, θ, q_1, q_2:
- Locations: $\theta_0 = 0$; $q_{10} = 0.00192$ m; $q_{20} = 0.00257$ m; $x_{s0} = 0.00903$ m
- Velocities: $\dot\theta_0 = 0$, $\dot q_{10} = 0$, $\dot q_{20} = 0$, $\dot x_{s0} = 0$

where: θ_0 is the initial swing angle of the lifting body and x_{s0} is the initial elongation of the spring:

$$x_{s0} = P_1/c = P_1\left(l_5 + s_{10} + s_{20} + s_0/n_p\right)/EF$$

rope with elastic modulus $E = 1{,}4.10^{11}$ N/m², rope diameter $d = 20$ mm, hoist multiplier $n_p = 2 q_{10}$, q_{20} is the initial static settlement of the ground at the front and rear outrigger positions, respectively.

$$q_{10} = N_1/c_1, q_{20} = N_2/c_2$$

where: N_1, N_2 is the total static pressure, determined from the initial static equilibrium condition:

$$N_{20} = 77.8 \text{ kN} \Rightarrow q_{20} = 0.00192 \text{ m and } N_{10} = 104.13 \text{ kN} \Rightarrow q_{10} = 0.00257 \text{ m}$$

Figure 3a shows the elastic vibration of the rope. During the period from 0 s to 20 s, the rope lengthens, so the static elongation gradually increases and elastic oscillation around that static strain. The next period oscillates around the constant static strain and fades out. Figure 3b indicates the oscillation of weight 1, the oscillation is stable after the motion stops, and the amplitude of the oscillation is about 1.50. This oscillation will fade if we add an air resistance factor.

Figures 4 and 5 present the deformation graphs of the ground and the total front and rear outrigger pressure. The ground deformation and this pressure depend on the movement of the boom and the shaking of load 1. This pressure changes relatively large in the following regions: The total pressure of the rear outrigger N_2 in the acceleration region from 0–3 s has a minimum value of about 68.3 kN and a maximum of 93.6 kN; it increases as the mechanism moves uniformly; in the speed reduction area from 17 s to 20 s, the minimum value is about 141.5 kN and the maximum is 152.4 kN; in the region of no

movement over 20 s, the minimum value is about 130.6 kN and the maximum is 147.2 kN. With total front outrigger pressure, the opposite rule.

The influence of the inclination angle changes on the dynamic response of the crane

Investigate the influence of the inclination angle of the boom on the oscillation. The parameters are taken as above, in which the angle of inclination of the boom is taken as

Figure 6 is a graph of rope strain. The magnitude of cable strain increases as the boom angle increases but the vibration amplitude decreases.

Figure 7 is the total front outrigger pressure, we see that the smaller the angle of inclination of the boom (corresponding to the increased reach), the lower the pressure of the front outrigger, in the case of a 30° tilt angle, this pressure is negative, that is, the crane has lost balance and overturned. Figure 8 is the total rear outrigger pressure.

a) Survey 2
b) Survey 3
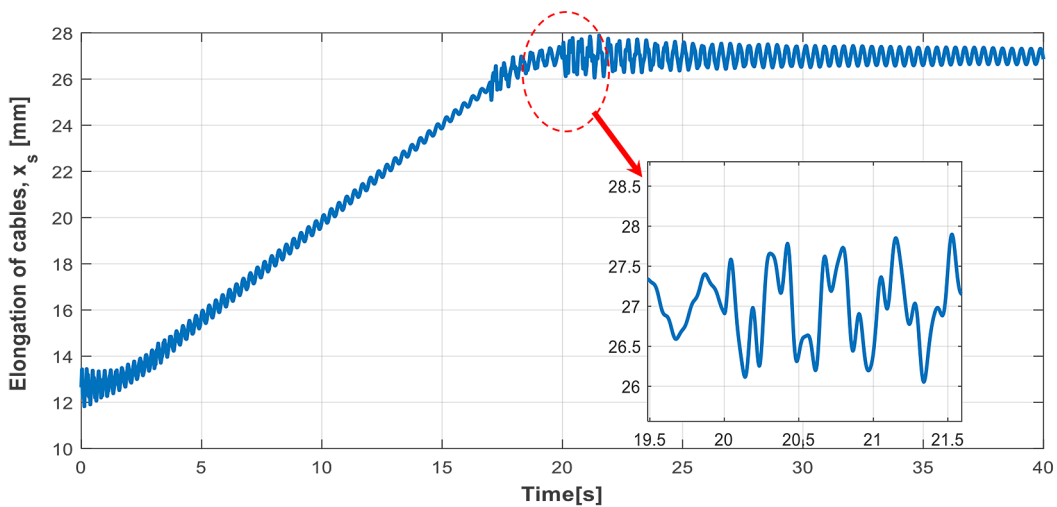
a) Elastic vibration of rope
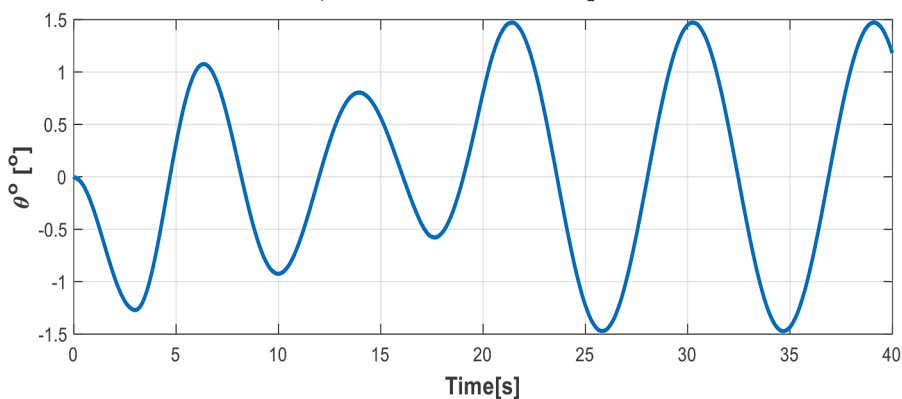
b) Vibration of a load 1

Figure 3. Vibration of rope and load 1, a) Elastic vibration of rope, b) Vibration of a load 1
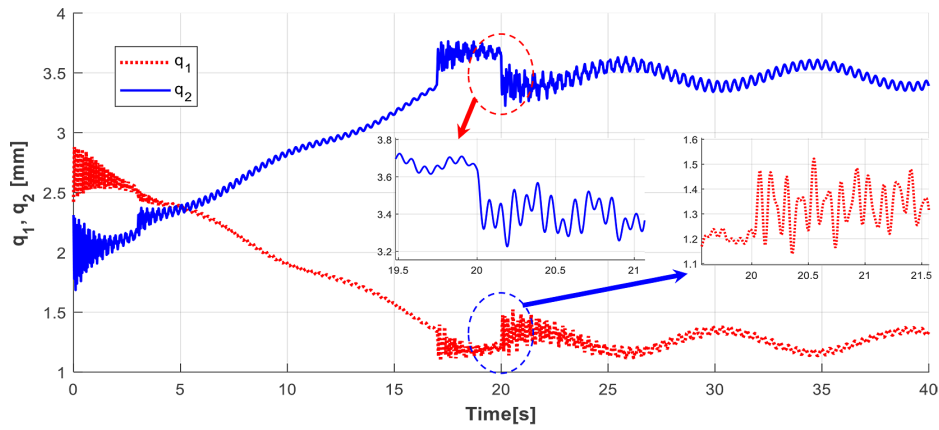
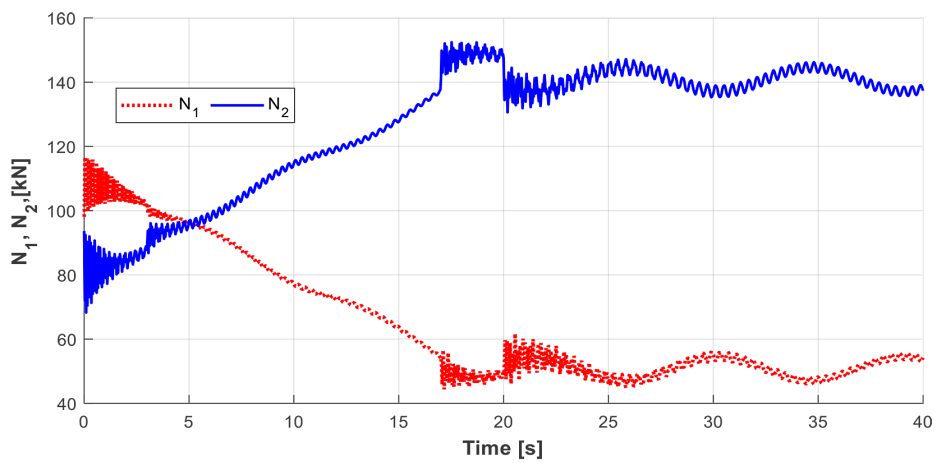**Figure 4.** Vibration of outrigger on front and rear

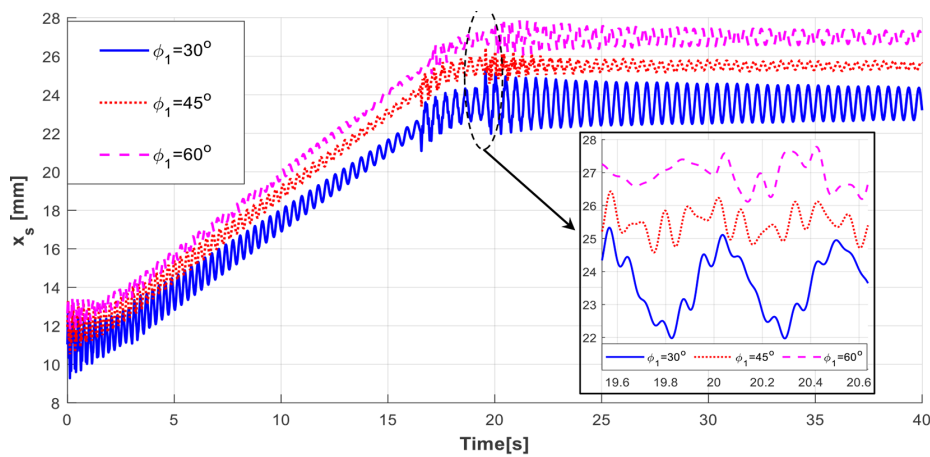**Figure 5.** Total front and rear outrigger pressure

Figure 6. Elastic vibration of the rope

Figure 9a is the shaking oscillation of the load, we see that in the case of an inclination angle of 45°, the amplitude of the shaking oscillation is larger than in the other two cases, so it also causes a larger pressure change than the other two cases remaining cases.

The influence of the changing speed of the boom length on the dynamic response of the crane

Investigate the effect of speed of change of boom length. When the changing speed of the length of the boom increases, the amplitude of
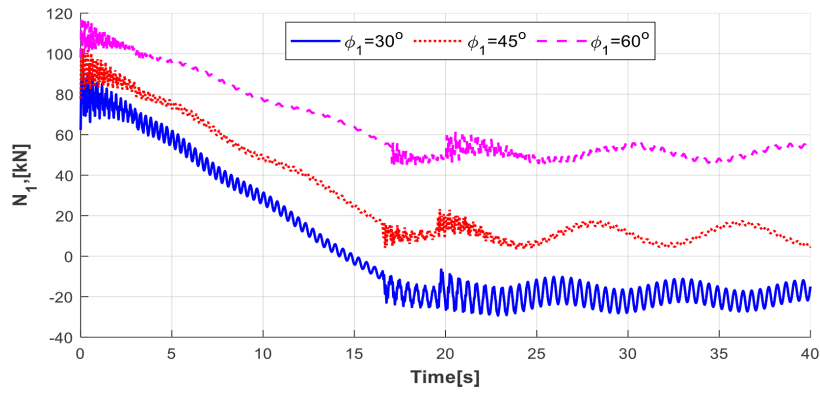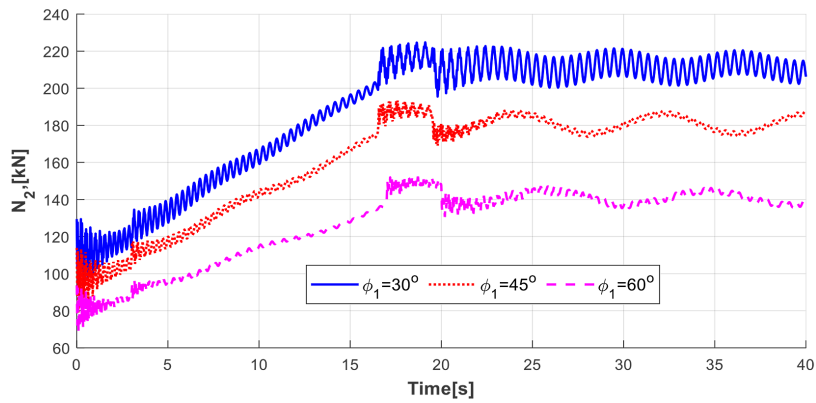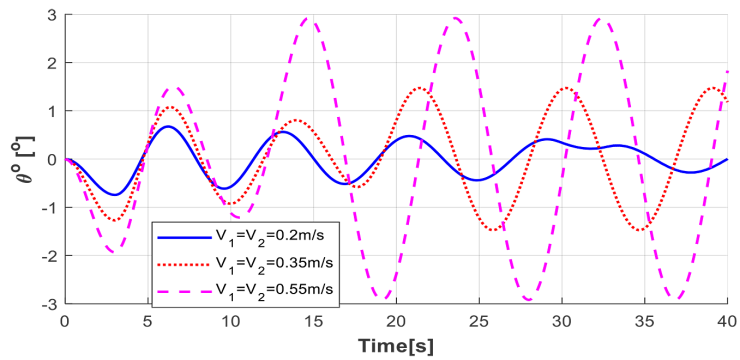
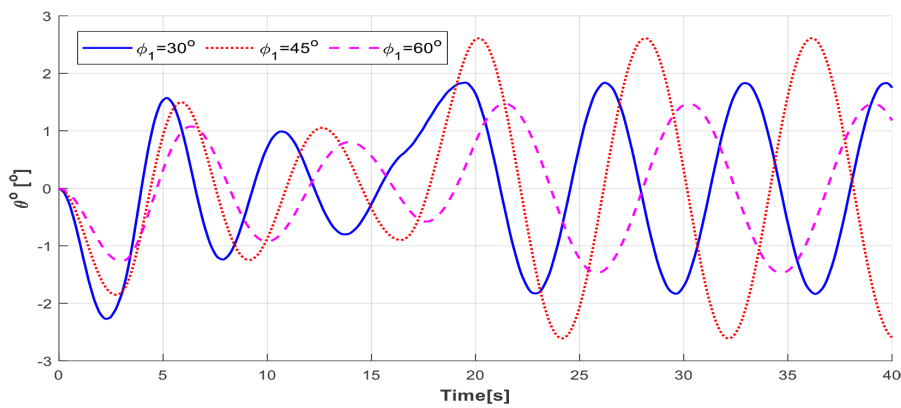**Figure 7.** Total front outrigger pressure

Figure 8. Total rear outrigger pressure

a) Survey 2

b) Survey 3

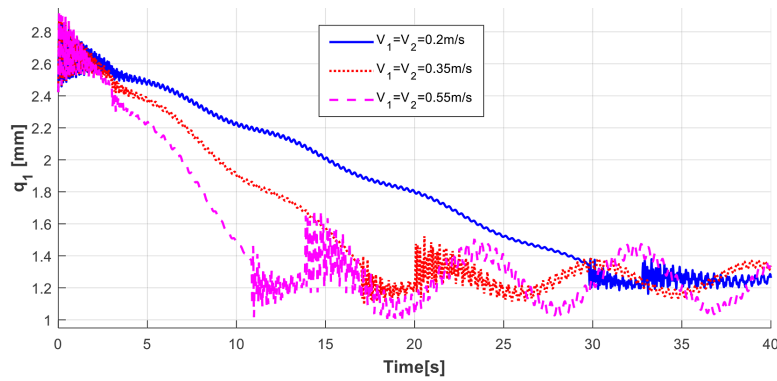**Figure 9.** Vibration of a load 1, θ (degree).

Figure 10. Vibration of the front outrigger

shaking oscillation increases accordingly, as shown in Figure 9b, the speed $V_1 = 0.2$ m/s, the swing amplitude is about 0.6°, the speed increases to $V_1 = 0.35$ m/s The shaking amplitude is about 1.5° and when $V_1 = 0.55$ m/s the shaking amplitude is about 3°. This shaking amplitude increases, causing the settlement vibration amplitude to increase accordingly as shown in Figure 10.

CONCLUSIONS

The process of designing and employing the truck crane always presents the problem of providing reliable and safe operation. Thus, there is a need to introduce new and improving previous mechanical models to describe the problems of exploitation more precisely. Such a contribution provides the possibility of introducing appropriate devices, measures, and procedures that will result in improving the safety of construction and the personnel in charge.

The article has modeled the dynamics of a truck crane and established a system of Equations describing it working in the plane when considering the deformation factors of the ground and rope.

Analyzed and surveyed in the working case when increasing the length of the boom in the article allows the following conclusions could be drawn:
1. The system of Equations describing the crane truck working in a plane is complicated if the elastic deformation of some parts such as lifting cables and the ground is considered. If we let these deformation components be zero, we will get the system of Equations of the crane truck when the parts are all solid.
2. During the working process, the influence of the moving factors, the tilt angle of the boom. These parameters will affect the swing of the

load, and the elastic vibration of the ground, thereby affecting the stability of the truck crane when operating. Several influences have been investigated by the article.
3. In the case of studying the effect of the boom length and its angle of inclination, the characterization of the changes in the vibration frequency and their values on the boom length was obtained. Similar vibrational frequencies with their slightly different varying characters were obtained for shorter boom lengths. The inclination angle of 45° results in the greatest shaking vibration compared to inclination angles of 30° and 60°. As the speed of boom length changes increases, the shaking amplitude increases correspondingly. The frequencies remain unchanged because the length of the lifting cable remains unchanged.
4. Based on the dynamic model built in the article, the study of the stability and control of the truck crane is completely feasible. Within the limits of this paper, these studies have not been presented.
5. Agreement in the obtained results indicates the correctness of the built models. Verification of the built models will be possible after conducting experimental research on the real object (on a truck crane).

REFERENCES

1. Umer K.H., Shah H. Advances in Industrial Control Dynamics and Control of Industrial Cranes. 2019.
2. Abdel-Rahman E.M., Nayfeh A.H., Masoud Z.N.

Dynamics and control of cranes: A review. JVC/ Journal Vib. Control. 2003; 9: 863–908. https://doi.org/10.1177/1077546303009007007

3. Cekus D., Gnatowska R., Kwiatoń P. Impact of Wind on the Movement of the Load Carried by Rotary Crane. Appl. Sci. 2019; 9. https://doi.org/10.3390/app9183842

4. Geisler, T., Sochacki W. Modelling and research into the vibrations of truck crane. Sci. Res. Inst. Math. Comput. Sci. 2011; 10: 49–60.

5. Taylor P., Mijailovi R. Modelling the dynamic behaviour of the truck-crane. Transport 2011, 26, 410–417. https://doi.org/10.3846/16484142.2011.642946

6. Trąbka A. Dynamics of telescopic cranes with flexible structural components. Int. J. Mech. Sci. 2014, 88, 162–174. https://doi.org/10.1016/j.ijmecsci.2014.07.009

7. Ilir D., Naser L. Truck mounted cranes during load lifting – dynamic analysis and regulation using modelling and simulations. Int. Sci. J. Mach. Technol. Mater. 2016, X, 12–15.

8. Sağirli A., Bočoçlu M.E., Ömürlü V.E. Modeling the dynamics and kinematics of a telescopic rotary crane by the bond graph method (Part I). Nonlinear Dyn. 2003; 33: 337–351. https://doi.org/10.1023/B:NODY.0000009929.80965.3b

9. Raftoyiannis I.G., Michaltsos G.T. Dynamic behavior of telescopic cranes boom. Int. J. Struct. Stab. Dyn. 2013; 13: 1350010-1-1350010–13. https://doi.org/10.1142/S0219455413500107

10. Liu S., Liu J., Zhang K., Meng L. The dynamic stability analysis of telescopic booms of the crane based on the energy method. IOP Conf. Ser. Mater. Sci. Eng. 2018. https://doi.org/10.1088/1757-899X/399/1/012033

11. Zheng Y., Wang D. Dynamic model studies of telescopic crane with a lifting and pulling load movement. Wirel. Pers. Commun. 2018; 102: 753–767. https://doi.org/10.1007/s11277-017-5098-y

12. Maczynski A., Wojciech S. Dynamics of a mobile crane and optimisation of the slewing motion of its upper structure. Nonlinear Dyn. 2003; 32: 259–290. https://doi.org/10.1023/A:1024480318414

13. Esqué S., Raneda A., Ellman A. Techniques for studying a mobile hydraulic crane in virtual reality. Int. J. Fluid Power 2003; 4: 25–35. https://doi.org/10.1080/14399776.2003.10781163

14. Hera P. L., Mettin U., Manchester I.R., Shiriaev A. Identification and control of a hydraulic forestry crane. In: Proceedings of the 17th World Congress the International Federation of Automatic Control, Seoul, Korea, 6–11 July 2008. https://doi.org/10.3182/20080706-5-kr-1001.00389

15. Sochacki W., Tomski L. Free and parametric vibration of the system: telescopic boom - hydraulic cylinder (changing the crane radius). Arch. Mech. Eng. 1999; 46: 257–271.

16. Bold M., Garus S., Sochacki W. Damped vibrations of telescopic crane boom. In: 24th International Conference Engineering Mechanics, Svratka, Czech Republic, 14–17 May 2018. https://doi.org/10.21495/91-8-101

17. Qian J.B., Bao L.P., Yuan R.B., Yang X.J. Modeling and analysis of outrigger reaction forces of hydraulic mobile crane. Int. J. Eng. 2017; 30: 1246–1252. https://doi.org/10.5829/ije.2017.30.08b.18

18. Kacalak W., Budniak Z., Majewski M. Computer aided analysis of the mobile crane handling system using computational intelligence methods. Adv. Intell. Syst. Comput. 2018; 662: 250–261. https://doi.org/10.5829/idosi.ije.2017.30.08b.18

19. Sun G., Kleeberger M., Liu, J. Complete dynamic calculation of lattice mobile crane during hoisting motion. Mech. Mach. Theory 2005; 40: 447–466. https://doi.org/10.1016/j.mechmachtheory.2004.07.014

20. Kjelland M.B., Hansen M.R. Using input shaping and pressure feedback to suppress oscillations in slewing motion of lightweight flexible hydraulic crane. Int. J. Fluid Power 2015; 16: 141–148. https://doi.org/10.1080/14399776.2015.1089071

21. Shabana A.A. Theory of Vibration. An Introduction. 1991; 1.